# Statistical Reliability and Measurement Characterization of Ultra-Thin Carbon Fibre Laminates under Quasi-Static Tension

Larry Hui[1,*], Maylee Tan[1], Skye Eleanor Heiles[1], Anuj Kakde[1], Alyn Panggabean[1], Kelin Eyvazi[2], and Hayden K. Taylor[1]

[1]Department of Mechanical Engineering, University of California, Berkeley, USA

[2]Department of Physics, University of California, Berkeley, USA

*Author to whom any correspondence should be addressed.

**E-mail:** larryhui7@berkeley.edu

**Keywords:** Carbon Fibre Laminate, Composites, Tensile Behavior, Weibull Statistic, Material Properties

**Abstract**

In this paper, we propose a statistical reliability framework for characterizing the tensile behavior of ultra-thin carbon fibre laminates under quasi-static loading using a standard gauge length of $7 \times 1$ inches, as specified by ASTM, where conventional testing assumptions and material property data are often inadequate. Quasi-static tensile tests were performed on 3-ply K13C2U carbon fibre laminates with a $0°/90°/0°$ layup, tested in both longitudinal and transverse orientations. Due to the brittle nature of the material and the limited specimen thickness, significant scatter in failure strength was observed. To quantify this variability, Weibull statistical analysis, bootstrap resampling, and non-parametric hypothesis testing were employed. The tensile strength distributions were found to be well described by a Weibull distribution, yielding shape parameters of 5.89 and 4.39 for the transverse and longitudinal orientations, respectively. Survival probability and hazard rate analyses further revealed distinct reliability regimes, identifying stress ranges associated with rapid increases in failure likelihood. A Kruskal–Wallis $H$ test confirmed a statistically significant dependence of tensile strength on fiber orientation. Comparison with manufacturer-reported properties highlighted discrepancies, underscoring the necessity of application-specific testing for ultra-thin laminate systems. These results demonstrate the importance of probabilistic characterization when designing load-bearing components from thin composite laminates.

## 1 Introduction

Carbon fiber laminates are critical in advanced engineering applications due to their excellent strength-to-weight ratio. In the development of the Electron-Ion Collider (EIC) at Lawrence Berkeley National Laboratory (LBNL), the carbon fiber laminates play a vital role as structural components in the detector. It is part of the collider's tracking and detection system, which is responsible for observing/analyzing particles produced in high-energy collisions. The laminates must provide structural rigidity to support the weight of the sensors and hardware without becoming misaligned or distorted/distorted while also being lightweight to avoid adding extra mass and compromising the collider's efficiency. Although carbon fiber laminates are widely used, there is limited empirical data on extremely thin K13C2U laminates and how orientation affects tensile performance under specific conditions.

Despite their widespread use, the tensile reliability of ultra-thin carbon fibre laminates is poorly characterized, particularly in regimes where conventional testing assumptions and bulk laminate property data may not apply. In this study, we investigate the quasi-static tensile performance of thin K13C2U carbon fibre laminates, with a specific focus on the influence of fibre orientation on tensile strength, stiffness, and failure variability. The original factorial experimental design considered both laminate thickness and orientation as independent variables; however, the present work isolates the effect of orientation to enable a more focused reliability analysis.

Quasi-static tensile tests were conducted using a displacement-controlled universal testing machine to ensure precise measurement of force, deformation, and fracture behavior. As directed by LBNL specifications, 3-ply K13C2U laminates with a $0°/90°/0°$ layup were manufactured and tested.

Specimens were cut both parallel (longitudinal) and perpendicular (transverse) to the primary fibre direction to assess orientation-dependent variability. Experimental results are compared against theoretical and manufacturer-reported properties to identify deviations arising from laminate thinness, testing constraints, and material variability. Beyond validation, this work provides practical guidance for the reliable use of ultra-thin K13C2U laminates in load-bearing applications where probabilistic failure behavior must be accounted for in design.

## 2 Material Methods

An Instron universal testing machine [6800 Series] (Instron, Norwood, Massachusetts) with the Wedge Action Tensile Grip as well as a 100 kN load cell was utilized to test the tensile strengths of the carbon fiber laminates as shown in Figure 1. The Instron was set to displace the specimens at a rate of 0.1 mm/min.


**Figure 1.** Quasi-static tensile testing setup using an Instron 6800 with wedge action tensile grips for thin carbon fibre laminate specimens.

### *2.1 Carbon Fiber Laminate Preparations*

The carbon fiber laminates are 11 × 1 inches, 3-ply, and 0°/90°/0° oriented. According to an LBNL specification sheet, the surface texture thickness of the specimen is 0.0700 mm on both sides, measured with a peel-ply surface. Each cure ply thickness is 23.9 $\mu$m, leading to a 3-ply laminate thickness of 71.6 $\mu$m. The samples are manufactured by debulking prepreg K13C2U cuts in the 0°/90°/0° orientation in a clean environment. The uncooked part is then placed in a vacuum bag with thermocouples. These bags are placed in an autoclave and baked under pressure to cure the resin. The cooked samples (cut into 12 × 12 squares) are then cut into 1 × 1 strips and sanded to remove any imperfections that could create a weak point.

50 of the 3-ply carbon fiber laminate specimens have been manufactured, along with 15 of the 15-ply carbon fiber laminate specimens. Tensile tests were performed on 20 specimens cut in the transverse direction and 14 specimens cut in the longitudinal direction. Complications in wedge manufacturing limited the amount of laminates tested.

### *2.2 Design and Manufacturing of the Wedges*

Due to the restrictions on the thickness of the corrugated carbon fiber laminates, wedges are needed to grip the samples for testing using an Instron. Wedges with specifications of 1.4 × 1 inches and a thickness of 0.06 inches, according to ASTM D3039 standards, were manufactured from stainless steel and bonded to the laminates with epoxy on both ends, allowing the wedges to be reused in future tests. Figure 2 shows toleranced drawings for coupons with tabs required for testing carbon-fibre laminates.

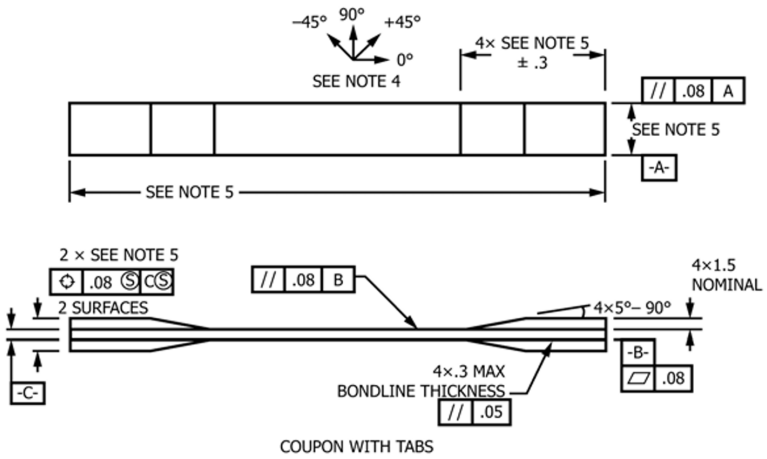


**Figure 2.** Geometry and dimensional specifications of the tensile coupon with bonded tabs used for quasi-static testing, adapted from ASTM D3039, showing fibre orientation reference, tab geometry, bondline thickness, and datum definitions.

Stainless steel wedges were cut into rectangles of the aforementioned dimensions ($1.4 \times 1.1 \times 0.06$ inches) and then set at an angle of $7^\circ$ and milled into a wedge shape. The wedges are then sanded, cleaned, and primed with scotchbrite for gluing onto the carbon fiber strips using Hysol 9309 two-part glue.

**Figure 3.** Close-up view of a thin carbon fibre laminate specimen, illustrating the laminate edge profile and ply stacking prior to tensile testing.

### *2.3 Alternative Designs of the Wedges*

As previously mentioned, the time required to manufacture and adhere the wedges to the specimens is hugely time-consuming. Alternative methods and approaches were considered and tried as outlined below.

The primary factor that hindered progress was the adherence process for the epoxy resins to cure overnight. An alternative was to use tape to secure the wedges with the specimen, and the Instron's compressive force would be enough to prevent slipping. However, during the tensile test, the force-displacement diagram showed significant slippage, rendering this method unreliable.

Another approach was to use sandpaper to grip the specimens rather than using wedges. Due to the thinness of the laminates, however, concerns arose regarding the jaws of the Instron being in contact with each other. A solution was to insert an aluminum shim between the jaws and the sandpaper to create more spacing; however, this proved unsuccessful due to the abrasive nature of the sandpaper, which wore down the specimen when gripped, weakening the laminates at their ends and subjecting the specimen to early fracture. The final method attempted was to manufacture the wedges from 1/16 inch plywood and then adhere them to the specimen using Krazy Glue. These wedges were designed and manufactured with a laser cutter, sanded to the exact specifications as the metal wedges, and, ostensibly, worked as well as the metal wedges, with the benefit of a quicker, more reusable end product.

### *2.4 Mechanical Testing and Clamps*

During tensile testing, one must be careful when loading the samples to ensure they do not rip along the grip due to the wedges' geometry and the fragility of the laminates. Once the upper fixture grips the specimen, it is crucial to protect it before engaging the lower grip to avoid any potential damage or misalignment. This protection ensures the specimen is stabilized adequately before the lower grip secures it, allowing for accurate and safe testing. Before the lower grip clamps the specimen, the Instron is zeroed such that the displacement and force readings are zero. Once the lower grip clamped the sample wedges, the force was again zeroed, resulting in a display reading of less than 5 N.

ASTM D3039/D3039M lists the procedure for inserting samples into the grips: to "align the long axis of the gripped specimen with the test direction" [1]. Each specimen was displaced at a rate of 0.1 mm/min until failure. Specimen failures are shown below in Figures 4, 5 and fall under 3 types of failure: i) Fracture due to stress concentrations in the clamps; ii) Two fractures along gauge length; iii) Single fracture in the middle of specimen.

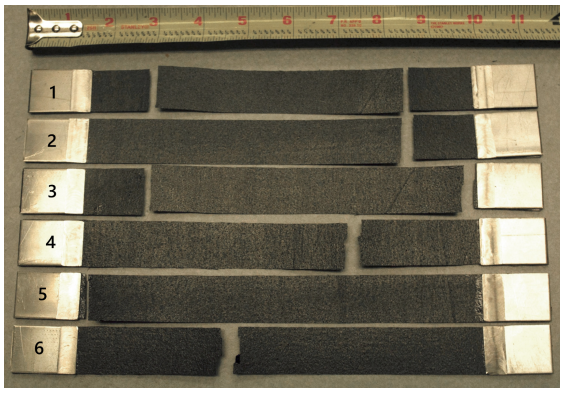


**Figure 4.** Representative carbon fibre laminate tensile specimens with bonded end tabs prior to testing. Specimens are labeled for identification, and a ruler is shown for scale.


**Figure 5.** *Continued.* Representative carbon fibre laminate tensile specimens with bonded end tabs prior to testing. Specimens are labeled for identification, and a ruler is shown for scale.

Due to updated facility safety restrictions implemented prior to the final testing phase, further mechanical testing of carbon fibre laminates was not permitted. As a result, additional experiments on the thicker 15-ply laminates could not be completed.

## 3 Weibull Statistical Analysis

Unlike metals, carbon fiber laminates are brittle and exhibit low fracture toughness. Similar to other brittle materials, plastic deformation at the crack tip is very limited, and failure therefore occurs by fast fracture [2]. While similar formulations have been widely applied to the study of brittle materials, including carbon fibers, the selection of an appropriate statistical model to describe the distribution of tensile failure strengths nevertheless requires justification.

Weibull analysis, which accounts for inherent data randomness, is therefore commonly employed for fragile materials, as the statistical distribution of damage plays a central role in the fracture process [3]. Variations in crack length among nominally identical specimens consequently lead to statistical variability in tensile strength, which can be approximated by [2].

$$\sigma_{\mathrm{TS}} \approx \frac{K_{IC}}{\sqrt{\pi a_c}} \tag{1}$$

where $\sigma_{\mathrm{TS}}$ denotes the tensile strength, $K_{IC}$ is the fracture toughness in mode I (tension) loading, and $a_c$ is the critical crack length. As a result, repeated tensile tests produce a distribution of strength rather than a single deterministic value.

To model this statistical variability in tensile strength, a Weibull distribution was adopted. The Weibull probability density function (PDF) is given by

$$f(\sigma) = \frac{m}{\lambda}\left(\frac{\sigma}{\lambda}\right)^{m-1} \exp\left[-\left(\frac{\sigma}{\lambda}\right)^{m}\right] \tag{2}$$

where $m$ is the Weibull shape parameter (modulus), which characterizes the scatter in strength, and $\lambda$ is the scale parameter corresponding to the characteristic tensile strength.

Determination of the Weibull shape parameter $m$ is necessary for estimating the survival probability, which can be expressed in simplified form as [2]

$$P_s(V) = \exp\left(-\frac{1}{\sigma_0^m V_0}\int_V \sigma^m \,\mathrm{d}V\right) = \exp\left[-\frac{V}{V_0}\left(\frac{\sigma}{\sigma_0}\right)^m\right] \tag{3}$$

where $\sigma_0$ is the characteristic strength and $V_0$ is a reference volume.

In general, at least 10 tensile tests are required to obtain a reasonable estimate of the Weibull modulus, while approximately 30 tests are recommended for statistically robust parameter estimation. Weibull parameters can be estimated using two common approaches. The first is a least-squares (LS) method, which linearizes the Weibull cumulative distribution function (CDF) by taking natural logarithms and performing linear regression,

$$F(x) = 1 - \exp\left[-\left(\frac{x}{\lambda}\right)^m\right] \tag{4}$$

$$\ln\big[-\ln\big(1 - F(x)\big)\big] = m\ln(x) - m\ln(\lambda) \tag{5}$$

while the second approach employs maximum likelihood estimation (MLE), which involves maximizing the likelihood function of the Weibull PDF [4],

$$\max_{m,\lambda} L(m,\lambda) = \max_{m,\lambda}\prod_{i=1}^{n} f(x_i;m,\lambda) \tag{6}$$

$$= \max_{m,\lambda}\sum_{i=1}^{n} \ln\left[\frac{m}{\lambda}\left(\frac{x_i}{\lambda}\right)^{m-1}\exp\left(-\left(\frac{x_i}{\lambda}\right)^m\right)\right] \tag{7}$$

In this paper, the LS approach is used to estimate Weibull parameters due to its numerical stability and simplicity for limited sample sizes. For goodness-of-fit evaluation using the Kolmogorov-Smirnov (KS) test, MLE-based parameter estimates are employed. While both methods yield comparable results, MLE is asymptotically optimal and attains the Cramér-Rao lower bound, whereas the LS approach provides a computationally efficient and sufficiently accurate alternative for the present analysis.

### *3.1 Bootstrapping for Weibull Analysis*

In some circumstances, we can analytically determine the sampling distributions of a statistic. However, for many statistics of practical interest, such as the mean tensile strength considered in

this study, closed-form expressions for the sampling distribution are generally unavailable, as deriving such distributions becomes analytically intractable without imposing strong assumptions that may not be physically or statistically justified for composite materials.

Because the sample size for each laminate configuration is less than 30 independent and identically distributed (i.i.d.) specimens, we cannot invoke the central limit theorem reliably to approximate the sampling distribution as normal. Although Kolmogorov–Smirnov (KS) and Levene's tests (Section 4.3) support a Weibull model for the underlying strength distribution, the sampling distributions of Weibull parameter estimates, particularly the scale and shape parameters, are known to exhibit significant bias and variability at small sample sizes. Consequently, deriving an analytical sampling distribution using a MLE framework would be unpractical.

Thus, we resort to a simulation-based approach to estimate the sampling distribution and obtain statistically viable Weibull modulus and shape parameters. Ideally, a larger experimental dataset would have enabled direct empirical characterization; however, safety restrictions related to carbon fiber dust particle exposure prevented further specimen fabrication and testing. Bootstrapping, a Monte Carlo procedure, was used to estimate the distribution of the mean tensile strengths of the carbon fiber laminates. This approach is well suited to situations with no closed-form analytical solution or reliable normal approximation. We used the Monte Carlo algorithm for resampling, given a sample $\{x_1, \ldots, x_n\}$:

**Algorithm 1** Bootstrap Monte Carlo Resampling Procedure

**Require:** Original sample $\{x_1, x_2, \ldots, x_n\}$
**Require:** Number of bootstrap resamples $B$
**Ensure:** Bootstrap distribution of statistic $t(\cdot)$
1: **for** $b = 1$ to $B$ **do**
2: Draw a resample $\{x_{\pi(1)}, \ldots, x_{\pi(n)}\}$ with replacement, where $\pi(i) \sim \text{Uniform}\{1, \ldots, n\}$
3: Compute the bootstrap statistic $t^{(b)} = t(x_{\pi(1)}, \ldots, x_{\pi(n)})$
4: **end for**
5: **return** $\{t^{(1)}, t^{(2)}, \ldots, t^{(B)}\}$

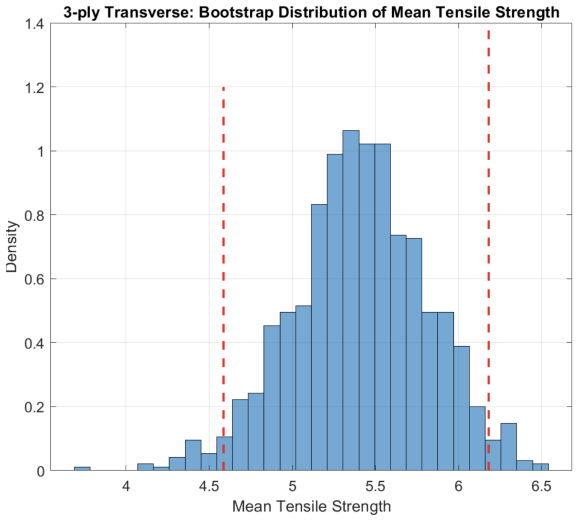


**Figure 6.** Bootstrapped sampling distribution of the mean tensile strength for 3-ply transverse carbon fibre laminates. The dashed red lines indicate the 95% confidence interval of the estimated mean.

Our bootstrapped data in Figure 6 show the density of estimated tensile strengths. We use these, in addition to the tested data, to estimate the Weibull shape parameters and validate our conclusions in lieu of additional experimental data. However, bootstrapping has limitations: the sample must be representative of the population, and any influential or high-leverage points in the sample can cause bias in the bootstrap distribution. Hence, the procedure will account for the variability and early fractures that may occur, and including outlier data points helps represent the data more accurately. We used bootstrap sampling to select two points for the transverse failure strength and six points for the longitudinal failure strength to perform the Kruskal–Wallis $H$ test.

## 4 Results and Discussion

### *4.1 Combined Stress-Strain Plot (3-ply transverse)*

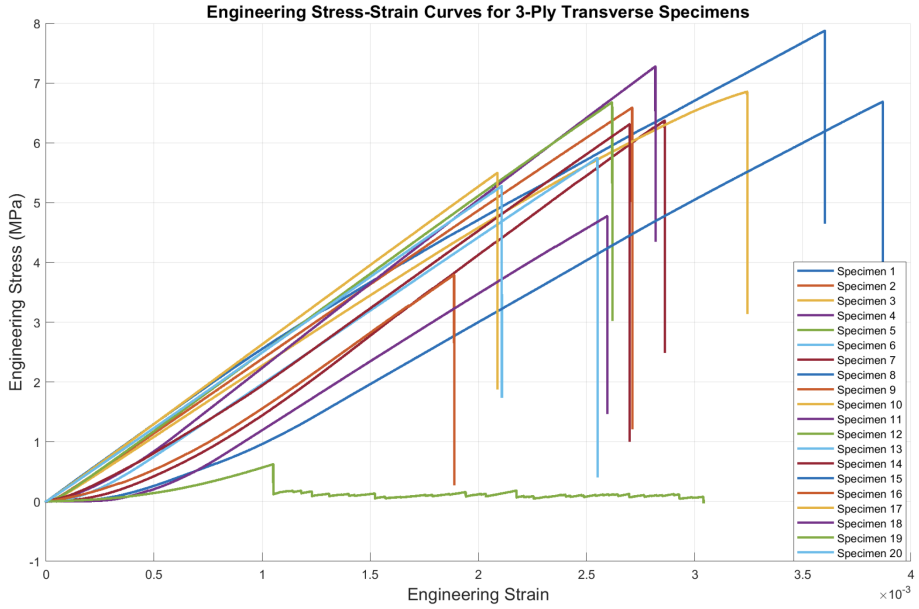


**Figure 7.** Engineering stress–strain curves for 3-ply transverse carbon fibre laminate specimens under quasi-static tensile loading. Individual curves correspond to separate specimens and show increased stiffness and strength relative to the transverse orientation.

In Figure 7, the strength-strain relationship of the 3-ply carbon fiber laminates under tensile stress is illustrated. These curves exhibit a two-phase behavior; initially, as tension is applied, the laminate exhibits a nearly straight-line response which represents the stretch and internal reconfiguration of its microstructure. As the specimens stretch, the fiber resists the pull with a more pronounced linear behavior until a sharp drop in stress at their respective fracture points, indicating the brittleness. The first phase, is a non-linear zone for strains between 0% and 0.06%, is followed by a second phase, a near-vertical drop in stress which is indicative of the specimen fracturing. The outliers in our transverse specimen data were specimens 5 and 19, which have a significantly lower stress/strain. These lower strain values are due to the premature failure of the specimens in which the extrinsic toughening mechanism of crack-bridging was at play, reducing crack growth.

### *4.2 Combined Stress-Strain Plot (3-ply longitudinal)*

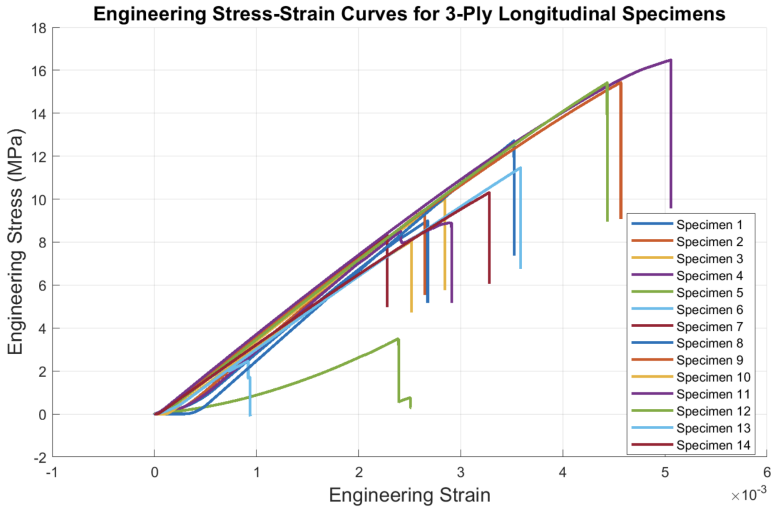


**Figure 8.** Engineering stress–strain curves for 3-ply longitudinal carbon fibre laminate specimens under quasi-static tensile loading. Individual curves correspond to separate specimens and show increased stiffness and strength relative to the transverse orientation.

In Figure 5, the strength-deformation relationship of the 3-ply longitudinal carbon fiber laminates under tensile stress is illustrated. They similarly exhibit a two-phase behavior as the transverse. However, there is a significantly higher yield strength reached; roughly on average twice that of the transverse data.

There are two outliers in our data, namely specimens 5 and 6. This is most likely due to the nature of the grips we were using. The metal wedges for specimens 5 and 6 were glued incorrectly. Not properly placing the wedges for the test could have caused there to be more stress at the ends of the grips which caused premature breaking of the specimen. It was observed that one of the wedges on specimen 5 was placed upside down, while specimen 6 was glued to a wedge with remnants of a previous carbon fiber laminate. Another possibility for the outliers could be from the glue itself. Not properly curing the glue could potentially lead to breaking.

### *4.3 Statistical Analysis of Specimens*

Following the experimentations, before conducting statistical tests, we need to verify the assumptions of normality and homogeneity of variances required for ANOVA. Additionally, the decision to use a model to depict the distribution of the strength at failure in carbon fibers deserves justification. The conformity of tensile strength data to a Weibull distribution was evaluated using a Kolmogorov-Smirnov (K-S) test. The Shapiro-Wilk test (SW) was employed to assess whether the tensile strength data follows a normal distribution. The test statistic was calculated as:

$$SW = \frac{\left(\sum_{i=1}^{n} a_i x_{(i)}\right)^2}{\sum_{i=1}^{n}(x_i - \overline{x})^2} \tag{8}$$

where $x_{(i)}$ is the ordered tensile strength data, $a_i$ are the weights based on normal distribution calculated based on Royston [5], $\overline{x}$ is the sample mean. For our tensile strength data, we determined that for the transverse laminates $SW = 0.84$, $p = 0.005$ at a significance level of 5%, which violates normality of the data as $p < 0.05$. Similarly for longitudinal, $SW = 0.94$, $p = 0.45$ at a significance level of 5%, $p > 0.05$. Therefore, ANOVA cannot be used, and an alternative method must be considered. The homogeneity of variances across groups was evaluated using Levene's test. Absolute deviations from group medians ($Zij = |x_{ij} - \hat{x}_i|$) were calculated, and the test statistic is computed as:

$$L = \frac{N-k}{k-1} \cdot \frac{\sum_{i=1}^{k} N_i(\overline{Z}_{i.} - \overline{Z_{..}})^2}{\sum_{i=1}^{k}\sum_{j=1}^{N_i}(Z_{ij} - \overline{Z}_{i.})^2} \tag{9}$$

where $Z_{i.}$ is the group mean of deviations, $Z_{..}$ is the overall mean of deviations, $N$ is the number of observations, and $k$ is the number of groups. For our data, $L = 4.1$. Since $L > F_{\alpha,k-1,N-k}$, the associated probability for the F-test is larger than 0.05. So, the assumption of homscedasticity was met. Finally, we performed a Kolmogorov-Smirnov (KS) test to check whether the tensile strength data follows a Weibull distribution; the empirical cumulative distribution function was compared to the Weibull CDF (3.3) where $m$ is the shape parameter, and $\lambda$ is the scale parameter. The K-S test statistic is calculated as follows:

$$D = \max_{x} |S(x) - F(x; m, \lambda)| \tag{10}$$

where $S(x)$ is the empirical cumulative distribution function (ECDF) defined as:

$$S(x) = \frac{\sum_{i=1}^{n} \leq X}{n}, \{x_1, x_2, \ldots, x_n\} \tag{11}$$

The KS test statistic was calculated with a corresponding $p$-value of 0.297 for the transverse samples and 0.723. Since $1 > \alpha = 0.05$, we fail to reject our null hypothesis that the tensile strength samples follow a Weibull Distribution and conclude that there is no significant evidence to suggest that the tensile strength data deviates from the Weibull distribution with the given parameters.

With the normality and homogeneity assumptions validated and the Weibull distribution confirmed as a good fit, subsequent analyses, including Weibull-based survival probability calculations, are deemed statistically robust; hence, these would provide a strong foundation for exploring the impact of laminate thickness and orientation on tensile strength and comparing experimental outcomes to manufacturer specifications. Given this, we plot the Weibull probability plot with the failure rate against the log of the fracture stress, as seen in Figure 9 and 10.

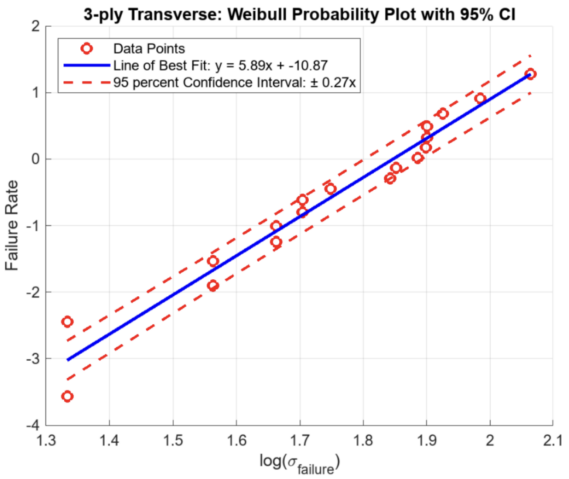


**Figure 9.** Weibull probability plot for 3-ply transverse carbon fibre laminate tensile strength data. Solid line is the maximum-likelihood Weibull fit, while dashed lines indicate the 95% confidence interval on the fitted distribution.

The yield strengths align well with the LS-line of best fit, indicating moderate consistency in the failure strengths. The slope of the line ($m = 5.89$) represents the Weibull shape parameter, which reflects relatively low variability in material performance. For a typical carbon fiber material, the Weibull modulus falls between 5 and 8 [6]. In this case, a modulus of 5.89 falls within the expected range. The characteristic strength $\sigma_0$, corresponding to a cumulative failure probability of 63.2%, can be derived from the regression equation, highlighting the material's typical failure threshold. The scatter of points around the line is minimal, suggesting that the material has a uniform quality, though any slight deviations could hint at variations due to imperfections or testing conditions. As shown by the 95% confidence interval, the uncertainty of this Figure 9 is ±0.27, determined using the propagation of uncertainty.

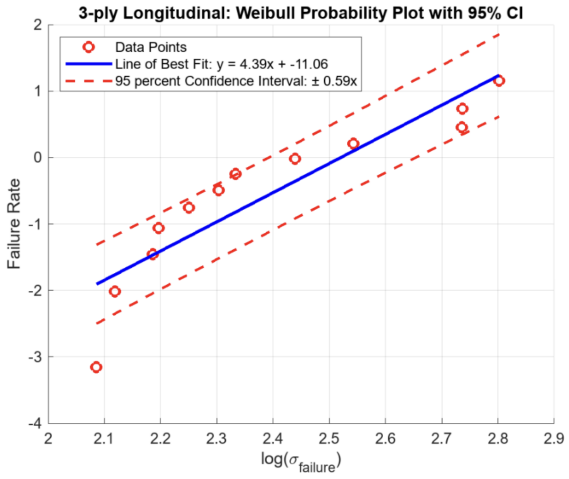


**Figure 10.** Weibull probability plot for 3-ply longitudinal carbon fibre laminate tensile strength data. Solid line is the maximum-likelihood Weibull fit, while dashed lines indicate the 95% confidence interval on the fitted distribution.

Similarly, in Figure 10, we have the probability plot for our longitudinal data. The yield strengths follow the LS-line of best fit, indicating solid consistency with a Weibull shape parameter of 4.39 which is slightly less than what is expected. The slight deviation could be due to issues during the setup of the experiment such as misalignment.

Plotting the hazard rate curve is helpful in indicating failure rate over time or strain. In plotting the failure stresses of each test against the hazard rate given the equation in (12) in which m is the Weibull shape parameter, S is the characteristic strength–the mean of the sorted failure stresses, and t are the tensile strengths.

$$HR = \frac{m}{S}\left(\frac{t}{S}\right)^{m-1} \tag{12}$$

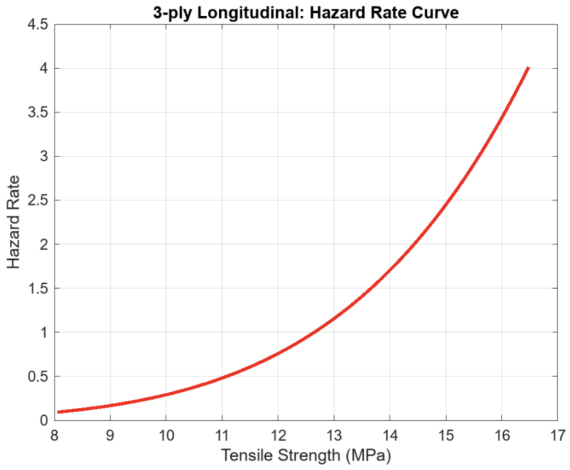


**Figure 12.** Estimated hazard rate as a function of tensile strength for 3-ply longitudinal carbon fibre laminate specimens, derived from the fitted Weibull distribution. The increasing hazard rate indicates a rising probability of failure with increasing applied stress.

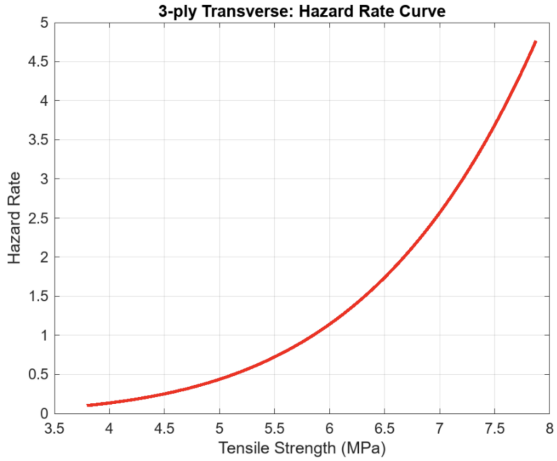


**Figure 11.** Estimated hazard rate as a function of tensile strength for 3-ply transverse carbon fibre laminate specimens, derived from the fitted Weibull distribution. The increasing hazard rate indicates a rising probability of failure with increasing applied stress.

The hazard rate curve for 3-ply transverse shown in Figure 11 suggests that staying within a lower tensile strength range would reduce the risks of failure. It can be observed that between 4 - 5 MPa, the hazard rate exponentially grew, thus suggesting that with higher tensile strengths, the specimens are more likely to fail. Similarly, the hazard rate curve for the 3-ply longitudinal is the exact same shape in Figure 12.

### *4.4 Kruskal-Wallis H Test for Comparison*

For robustness, it may be wise to do a two-way ANOVA to evaluate the effects of laminate thickness and fiber orientation on tensile strength, as well as their interaction. An appropriate statistical model can be defined as

$$\sigma_{ijk} = \mu + \alpha_i + \beta_j + (\alpha\beta)_{ij} + \epsilon_{ijk} \tag{13}$$

where $\sigma_{ijk}$ are the observed tensile strengths, $\mu$ is the overall mean tensile strength, $\alpha_i$ is the effect of the laminate thickness at the $i$-th level, $\beta_j$ is the effect of orientation at the $j$-th level, $(\alpha\beta)_{ij}$ is the interaction effect between the two variables, and $\epsilon_{ijk}$ is the random error term. However, due to complications with testing as outlined above in section 2.2 and a lack of normality for the tensile strength data, we resort to using non-parametric statistics, specifically the Kruskal-Wallis H Test. To evaluate if a transverse or longitudinal fiber orientation plays a significant role in the tensile strength of carbon fiber laminates, a Kruskal-Wallis H test was performed. This non-parametric test was chosen because it does not require assumptions of normality, making it suitable for data

that may not meet the conditions required for parametric tests, such as our one-way ANOVA. The null and alternative hypotheses for the Kruskal-Wallis test are:

$H_0$ : There is no difference in the distributions of tensile strength for transverse and longitudinal orientations.

$H_a$ :The distributions of tensile strength for transverse and longitudinal orientations are different.

The Kruskal-Wallis H test statistic is calculated using the following formula:

$$H = \frac{12}{n(n+1)} \sum_{i=1}^{k} \frac{R_i^2}{n_i} - 3(n+1) \tag{14}$$

where $n$ is the total number of observations across all groups, $k$ is the number of groups, which in this case are 2 (transverse, longitudinal), $n_i$ is the number of observations in the group, and $R_i$ is the sum of the ranks for the $i$-th group.

Firstly, the data from both fiber orientations were combined, sorted in ascending order, and assigned ranks. If we had the same tensile strength, we assigned them the average rank. Next, for each group, we summed the ranks to get Ri. Finally, we computed the test statistic. This test was performed in MATLAB(MathWorks, Natick, Massachusetts). The following table summarizes the test results.

**Table 1.** Kruskal-Wallis H Test results for the effect of orientation.

| Source | SS | DoF | MS | $\chi^2$ | $p$-value |
|---|---|---|---|---|---|
| Orient. | 2624.4 | 1 | 2624.4 | 19.21 | $1.1 \times 10^{-5}$ |
| Error | 2702.6 | 38 | 71.12 | — | — |
| Total | 5327.0 | 39 | — | — | — |

At a significance level of 5%, since the $p$-value is significantly smaller, we reject the null hypothesis. This indicates that there is a statistically significant difference in the tensile strength distributions between the transverse and longitudinal orientations of the carbon fiber laminates. This demonstrates that the direction of fiber orientation plays a significant role in influencing the tensile strength.

Practically, this would make sense since if fibers are aligned with the applied load direction, they are able to withstand more. By utilizing fibers with a weak matrix, when the matrix fails, the fibers are left intact spanning behind the crack tip and can act as bridges to inhibit crack opening [4]. In the longitudinal configuration, if the crack propagates from the side, crack bridging occurs from 2 layers which would allow for much more load to be passed through the fibers before breaking them. In the transverse configuration, the crack would be parallel to the fibers so it only has one layer of fibers to help bridge the crack which implies the yield strength and fracture strength will be lower.

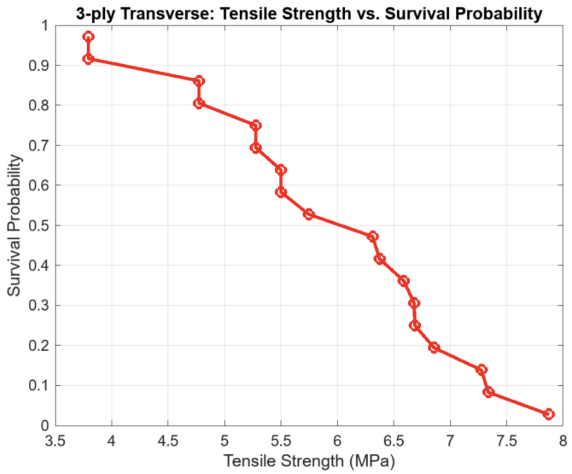


**Figure 13.** Empirical survival probability as a function of tensile strength for 3-ply transverse carbon fibre laminate specimens. The survival function illustrates the decreasing probability of specimen survival with increasing applied stress.

An additional reliability-based analysis was performed by examining tensile strength as a function of survival probability. The probability of failure was estimated using the median rank approximation,

$$F = \frac{k - 0.5}{n} \tag{15}$$

where $n$ is the total number of specimens and $k$ is the ordered failure index, ranging from 1 to $n$. The corresponding survival probability was then computed as

$$S = 1 - F \tag{16}$$

where $S$ denotes the probability that a specimen survives a given applied stress. The experimentally measured failure stresses were ranked in ascending order and plotted against the corresponding survival probabilities, yielding the tensile strength–survival probability relationship shown in Figure **??**. This representation complements the hazard rate analysis by providing an intuitive view of specimen reliability across the stress range. At lower tensile strengths (approximately 4–5 MPa), the survival probability remains high, indicating a low likelihood of failure. In the intermediate stress range of roughly 5–6 MPa, the survival probability decreases sharply, marking a transition region where failure becomes significantly more likely and conservative design margins are warranted. Beyond 6 MPa, the survival probability is low, indicating that failure is highly probable at these stress levels.

### *4.5 Comparison to Manufacturers' Claim*

In the previously mentioned specification sheet provided by LBNL, we are provided with known variables such as the fiber axial modulus, fiber transverse modulus, matrix modulus, fiber Poisson ratio, and matrix Poisson ratio. If the tensile test is along the 0° fiber, it is in the longitudinal direction. Whereas if the tensile test is along the 90° fiber, it is in the transverse direction. With the experimental data that has been acquired in the longitudinal and transverse direction, we are able to compare the modulus calculated from the manufacturer's data in Table 2. with the mean of the modulus in the transverse and longitudinal direction determined by our experimental data.

**Table 2.** Material properties and laminate configuration for the carbon fibre composite specimens.

| Property | Value |
|---|---|
| Fiber Type | K13C2U |
| Resin Mass Fraction ($M_m$) | 41% |
| Fiber Areal Weight (FAW) | 45 gsm |
| Void Fraction ($V_v$) | 0.5% |
| Surface Texture Thickness (Peel Ply) | 70 $\mu$m |
| Number of Layers | 3 |
| Layer Orientation | 0/90/0 |
| Fiber Axial Modulus ($E_{1f}$) | 896 GPa |
| Fiber Transverse Modulus ($E_{2f}$) | 7 GPa |
| Fiber Poisson's Ratio ($\nu_{12f}$) | 0.3 |
| Fiber Density ($\rho_f$) | 2.19 g/cm$^3$ |
| Matrix Modulus ($E_m$) | 4.4 GPa |
| Matrix Poisson's Ratio ($\nu_m$) | 0.35 |
| Matrix Density ($\rho_m$) | 1.17 g/cm$^3$ |

The fiber volume fraction is given by

$$V_f = \frac{1 - V_v}{1 + \frac{\rho_f (M_m)}{\rho_m (1 - M_m)}} \tag{17}$$

The matrix volume fraction is given by

$$V_m = 1 - V_f - V_v \tag{18}$$

The composite modulus in the transverse direction is given by

$$E_{22} = \frac{E_{2f}\sqrt{V_f} + E_m(1 - \sqrt{V_f})}{\sqrt{V_f}} + \frac{1 - \sqrt{V_f}}{E_m} \tag{19}$$

The calculations based on the manufacturer's specifications for uni-ply K13C2U yield the following values: $Vf = 43.2\%$, $V_m = 56.3\%$, and$E_{22} = 5.4$ GPa/mm. The laminate modulus for the calculated from these values for the $0°/90°/0°$ layup is is 133.8 GPa/mm. The calculated laminate thickness is 71.6 $\mu$m, so the calculated modulus for a laminate of our thickness would be 9.6 GPa. Meanwhile, the experimental mean composite modulus in the transverse direction is given by

$$\overline{E}_{22} = \frac{1}{n}\sum_{i=1}^{n} E_{22,i} \tag{20}$$

where $n = 18$ because specimens 5 and 19 are excluded. The experimental mean transverse modulus $\overline{E}_{22}$ is 2.23 GPa. The composite modulus in the longitudinal direction is given by

$$E_{11} = (1 - w)E_{1f}V_f + E_m V_m \tag{21}$$

$w$ is the weave stiffness reduction factor. As provided by LBNL, $w = 0\%$. The experimental mean composite modulus in the longitudinal direction is given by

$$\overline{E}_{11} = \frac{1}{n}\sum_{i=1}^{n} E_{11,i} \tag{22}$$

where $n = 12$ since specimens 5 and 6 are excluded because the glue was incorrectly applied to the wedges; one was glued upside down, and the other was glued to remnants of carbon fiber stuck to the laminate. This led to early slipping. The calculated longitudinal modulus is 390 GPa/mm based on the manufacturer's data. Similarly to before, this corresponds to a 262.2 GPa/mm laminate modulus which corresponds to a 18.8 GPa modulus for our laminate thickness (71.6 $\mu$m). The experimental mean longitudinal modulus is $\overline{E}_{11}$ is 3.33 GPa.

The thickness of our manufactured laminates happened to be very similar to the average thickness that we had calculated from the manufacturer specifications (71.6 $\mu$m $\sim$ 61.3 $\mu$m). Based upon that average thickness, the experimental modulus in the longitudinal direction is 54.3 GPa/mm and 36.4 GPa/mm in the transverse. Although the experimental moduli are the same order of magnitude as the calculated moduli, there are significant enough differences to raise suspicions about errors in the manufacturing and testing process as well as the state of the prepreg used:

Our primary hypothesis for the difference in the experimental versus calculated moduli values is the state of the carbon fiber. The K13C2U we used was expired, and therefore dry. This in and of itself could cause the laminate to cure poorly, leading to a less stiff laminate. This fact also affected the manufacturing process as it is difficult to lay up dry prepreg because it doesn't fully stick to itself properly in the debulking process. This too could have caused weaknesses in the laminate. Another hypothesis surrounding the discrepancy in the moduli is the influence of the wedges on the stress distributions, as the ASTM standard is for samples of at least 1 mm thickness. Different grip strategies could be explored for better results. The discrepancy could also be attributed to the calibration of the Instron, which was out of our control to test and recalibrate as it is property of UC Berkeley, and being used by other students.

## 5 Conclusion

Thus far, one can conclude that the transverse specimens will survive at the lower tensile strength range of 0 to $4.5 \pm 0.5$ MPa while they are more likely to break and fail in the higher ranges of the tensile strength: $< 6$ MPa. Likewise, for the longitudinal specimens, they have a wider range of service ranging from 0 to $13 \pm 0.5$ MPa on average.

Experimental data shows that the composite modulus in the transverse direction is 2.23 GPa, and the experimental longitudinal modulus is 3.33 GPa. These values are different from the calculated values, but are of the same order of magnitude. Our findings suggest that laminate orientation is a statistically significant factor dictating tensile strength, aligning with the structural role of fibers in resisting crack driving forces. These findings highlight the critical importance of fiber orientation in the design of load-bearing components, especially in optimizing material performance under tensile loads. Discrepancies between experimental and manufacturer data illustrate the importance of application-specific testing and validation.

Further studies could investigate the interaction between thickness and orientation of laminates or underlying causes of composite modulus discrepancies through testing conditions or manufacturing variability. Exploring other types of orientations at offset angles such as 45°, or hybrid laminates. These could all lead to invaluable insight for performance optimization and engineering.

## 6 Acknowledgements

We would like to acknowledge and thank the Hesse Hall Machine Shop staff: Daniel Paragas, Mike Neufer, and Tom Clark in assisting with our usage of the Instron. We would also like to thank Professor Hayden Taylor and our GSI, X Sun. This experimentation project would not have been possible without their guidance and direction.

Lastly we would like to thank the Lawrence Berkeley National Laboratory researchers, employees, scientists, and staff in collaboration with Skye Heiles for the manufacturing and fabrication of the specimens.

## Conflict of Interest

The authors declare no conflict of interest.

## References

[1] ASTM International. *ASTM D3039/D3039M-17: Standard Test Method for Tensile Properties of Polymer Matrix Composite Materials*. ASTM International, West Conshohocken, PA. Accessed: YYYY-MM-DD. 2017. DOI: 10.1520/D3039_D3039M-17.

[2] Michael F. Ashby and David R. H. Jones. *Engineering Materials 2: An Introduction to Microstructures and Processing*. 4th ed. Elsevier/Butterworth-Heinemann, 2013.

[3] I. Dembri et al. "Tensile Behavior and Statistical Analysis of Washingtonia Filifera Fibers as Potential Reinforcement for Industrial Polymer Biocomposites". In: *Journal of Natural Fibers* 19.16 (2022), pp. 14839–14854. DOI: 10.1080/15440478.2022.2069189.

[4] A. G. Evans. "Perspective on the development of high toughness ceramics". In: *Journal of the American Ceramic Society* 73 (1990), pp. 187–206.

[5] Patrick Royston. "Approximating the Shapiro–Wilk W-test for non-normality". In: *Statistics and Computing* 2 (1992), pp. 117–119.

[6] Francisco Mesquita et al. "Tensile Properties of Single Carbon Fibers Tested with Automated Equipment". In: *Proceedings of ICCM22*. Available at ICCM22 proceedings site. 2022. URL: https://iccm-central.org/Proceedings/ICCM22proceedings/.